ORNL/TM-5329

Cy 1

Mechanical Property Correlations for 2¼ Cr-1 Mo Steel in Support of Nuclear Reactor Systems Design

M. K. Booker
T. L. Hebble
D. O. Hobson
C. R. Brinkman

[redacted]

OAK RIDGE NATIONAL LABORATORY
OPERATED BY UNION CARBIDE CORPORATION FOR THE ENERGY RESEARCH AND DEVELOPMENT ADMINISTRATION

Printed in the United States of America. Available from
the Energy Research and Development Administration,
Technical Information Center
P.O. Box 62, Oak Ridge, Tennessee 37830
Price: Printed Copy $4.00 ; Microfiche $2.25

ORNL/TM-5329
UC-79b, -h, -k
(Liquid Metal Fast
Breeder Reactors)

Contract No. W-7405-eng-26

METALS AND CERAMICS DIVISION

MECHANICAL PROPERTY CORRELATIONS FOR 2 1/4 Cr-1 Mo STEEL IN SUPPORT OF NUCLEAR REACTOR SYSTEMS DESIGN

M. K. Booker, T. L. Hebble, D. O. Hobson, and C. R. Brinkman

JUNE 1976

OAK RIDGE NATIONAL LABORATORY
Oak Ridge, Tennessee 37830
operated by
UNION CARBIDE CORPORATION
for the
ENERGY RESEARCH AND DEVELOPMENT ADMINISTRATION

CONTENTS

MECHANICAL PROPERTY CORRELATIONS FOR 2 1/4 Cr-1 Mo STEEL IN SUPPORT OF NUCLEAR REACTOR SYSTEMS DESIGN

M. K. Booker, T. L. Hebble, D. O. Hobson, and C. R. Brinkman

ABSTRACT

In recent years, 2 1/4 Cr-1 Mo steel has gained worldwide importance as a structural material for use in steam generators. Therefore, it is important that the mechanical properties of this material be understood in some detail. A large collection of mechanical properties data for this material has been compiled from the literature and from private sources. Analysis of these data has yielded mathematical descriptions of the tensile, creep, fatigue, and impact properties of annealed and isothermally annealed 2 1/4 Cr-1 Mo steel. Where appropriate, statistical analysis has been performed to yield estimates of possible variations in behavior. The final results represent a comprehensive description of the mechanical behavior of the material. This description makes a large contribution to the characterization required for use of 2 1/4 Cr-1 Mo steel in the construction of nuclear systems.

INTRODUCTION

The design of modern nuclear reactor systems involves both the use of advanced analytical techniques and extensive information about the mechanical behavior of structural materials in order to meet increasingly stringent reliability requirements aimed toward better economics. In recent years, 2 1/4 Cr-1 Mo steel has been promoted worldwide as a structural material for use in nuclear steam generator systems, both in evaporators and in superheaters. In some cases, the long- and short-term mechanical properties of this material are not satisfactorily characterized for present design needs, and research is in progress to generate needed data. However, these data must be systematically presented in formats that are useful to designers. This paper presents an analysis of the tensile, creep, creep-rupture, fatigue, and impact properties of 2 1/4 Cr-1 Mo steel.

DATA USED

To determine general trends in mechanical properties and to assess the statistical variability in these properties, a large data base was needed. Data were assembled from the literature,[1–8] from private sources,[9–13] and from data obtained through the Mechanical Properties Data Center[14] and the Oak Ridge National Laboratory Mechanical Properties Data Storage and Retrieval System (DSRS).[15] Only data from tests conducted in air on annealed or isothermally annealed material were considered,

---

[1]W. F. Simmons and H. C. Cross, *Report on the Elevated-Temperature Properties of Chromium-Molybdenum Steeels, ASTM Data Ser. Publ.* DS-6, ASTM, Philadelphia, 1953.

[2]J. A. Van Echo and W. F. Simmons, *Supplemental Report on the Elevated-Temperature Properties of Chromium-Molybdenum Steels, ASTM Data Ser. Publ.* DS-6-S1, ASTM, Philadelphia, 1966.

[3]G. V. Smith, *Supplemental Report on the Elevated-Temperature Properties of Chromium-Molybdenum Steel (an Evaluation of 2 1/4 Cr-1 Mo Steel), ASTM Data Ser. Publ.* DS-6-S2, ASTM, Philadelphia, 1971.

[4]A. O. Schaefer, ed., *Symposium on 2 1/4 Chrome 1 Molybdenum Steel in Pressure Vessels and Piping,* ASME, New York, 1971.

[5]A. O. Schaefer, ed., *Current Evaluation of 2 1/4 Chrome 1 Molybdenum Steel in Pressure Vessels and Piping,* ASME, New York, 1972.

[6]R. L. Klueh, *Effect of Carbon on the Mechanical Properties of 2 1/4 Cr-1 Mo Steel,* ORNL-4922 (November 1973).

[7]*Data Sheets on the Elevated-Temperature Properties of 2 1/4 Cr-1 Mo Steel for Boiler and Heat Exchanger Seamless Tubes (STBA24)*, NRIM Creep Data Sheet No. 3, National Research Institute for Metals, Tokyo, Japan, 1972.

[8]*The Data of Short Time Tensile Properties of 2.25 Cr-1 Mo Steel at Elevated Temperature,* TD-47040, Nippon Kokan K. K., 1972.

[9]*The Data of Creep Rupture Properties of 2.25 Cr-1 Mo Steel,* TD-47039, Nippon Kokan K. K., 1972.

[10]Babcock and Wilcox Corporation Research Center, private communication, 1974.

[11]Combustion Engineering Corporation, private communication, 1974.

[12]D. I. Roberts and J. R. Ellis, General Atomics Corporation, private communication, 1975.

[13]R. L. Klueh, D. A. Canonico, and W. J. Stelzman, Oak Ridge National Laboratory, private communication, 1974.

[14]Data obtained from the Mechanical Properties Data Center, Traverse City, Mich., 1974.

[15]M. K. Booker and B.L.P. Booker, "Development and Implementation of a Mechanical Properties Data Storage and Retrieval System," ORNL/TM-5330 (to be issued).

although various annealing treatments were admitted. Typical treatments include:
Anneal — Austenitize at 927°C for 1 hr; furnace cool to 450°C; air cool to room temperature.
Isothermal anneal — Austenitize at 927°C for 1 hr; furnace cool to 704°C; hold 2 hr; furnace cool to room temperature.
Other restrictions on material considered included: room temperature ultimate tensile strength ⩾ 414 MPa (60 ksi); room temperature 0.2% offset yield strength ⩾ 207 MPa (30 ksi); carbon content 0.07 to 0.15%; chromium content 2.0 to 2.5%; and molybdenum content 0.9 to 1.1%. These restrictions are a subset of those given in standard materials specifications in the United States.[16,17] Finally, various product forms are represented, including bar, rod, tube, pipe, and plate.

TENSILE PROPERTIES

Short-term monotonic tensile data are directly applicable in setting design stress intensity limits, and they also lend insight into the general flow and failure characteristics of a material. The true stress-plastic strain behavior of this material as a function of temperature and strain rate has been analyzed by Klueh and Hebble,[18] who found that of several models fit to the data, the Voce equation[19] provided the best results overall.

Strength Properties

Tensile strength properties which have been investigated include the proportional limit (PL), 0.2% offset yield strength (YS), ultimate tensile strength (UTS), and true fracture stress (TFS). These properties were assumed to be describable by polynomials in temperature. Then, the order of polynomial was chosen in each case to provide the best balance of fit to the data and simplicity. The results of these analyses are shown in Figs. 1–4, including data and curves of expected values and upper and lower central tolerance limits. Assuming a normal distribution of the dependent variable about the predicted values, these limits

---

[16] *1974 ASME Boiler and Pressure Vessel Code, Section III, Nuclear Power Plant Components*, ASME, New York, 1974.

[17] *Interpretations of the ASME Boiler and Pressure Vessel Code, Code Case 1592*, ASME, New York, 1974.

[18] R. L. Klueh and T. L. Hebble, *A Mathematical Description for the Stress-Strain Behavior of Annealed 2 1/4 Cr-1 Mo Steel*, ORNL-TM-4928 (June 1975).

[19] E. Voce, "The Relationship Between Stress and Strain for Homogeneous Deformation," *J. Inst. Met.* 74: (1948).

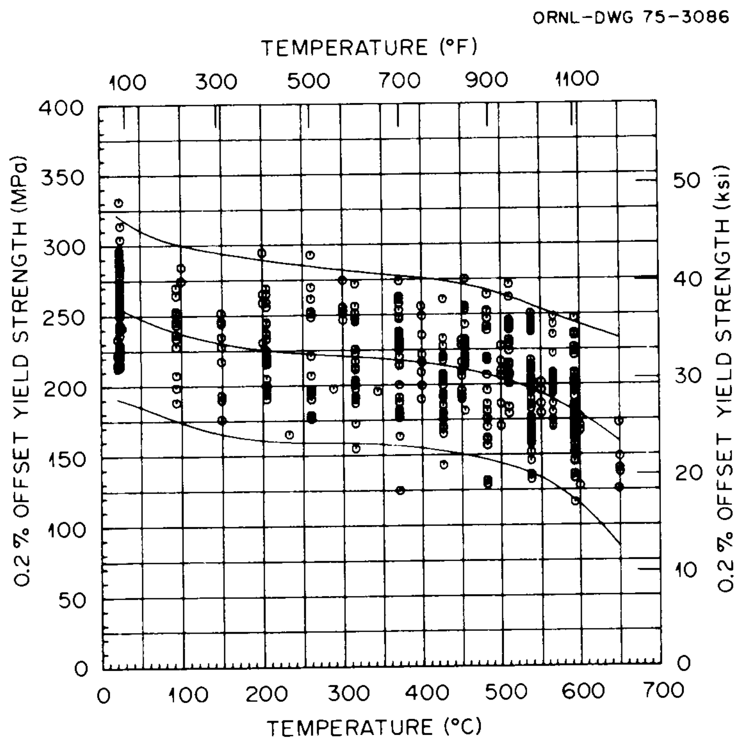

Fig. 1. 0.2% Offset Yield Strength vs Temperature, Including a Mean Regression Curve and Upper and Lower Tolerance Limits (P = 0.90, λ = 0.95).

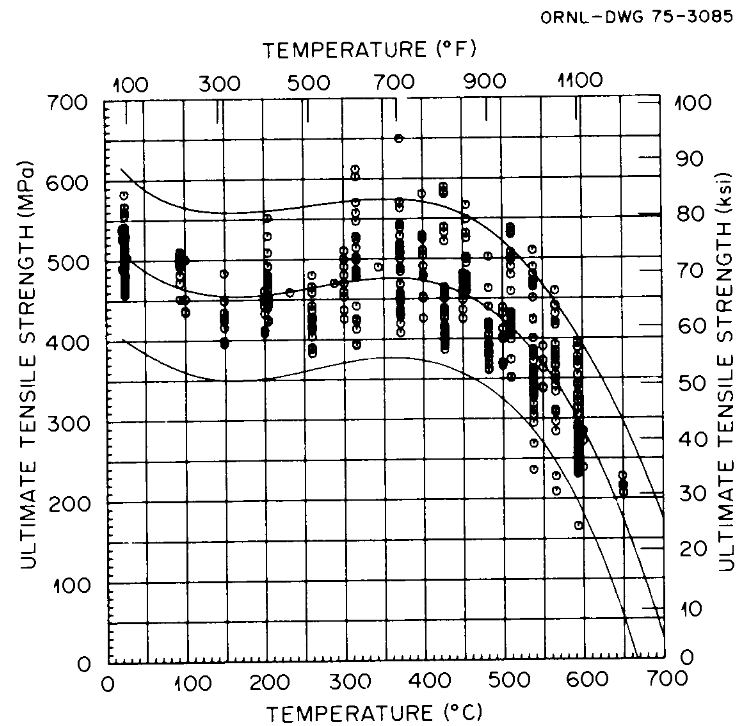

Fig. 2. Ultimate Tensile Strength vs Temperature, Including a Mean Regression Curve and Upper and Lower Tolerance Limits (P = 0.90, λ = 0.95).

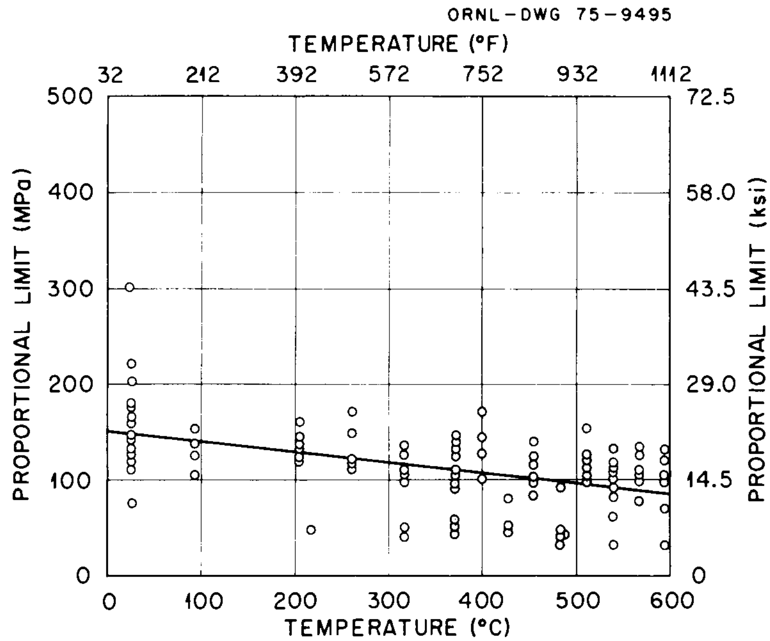

Fig. 3. Proportional Limit vs Temperature, Including a Mean Regression Line.

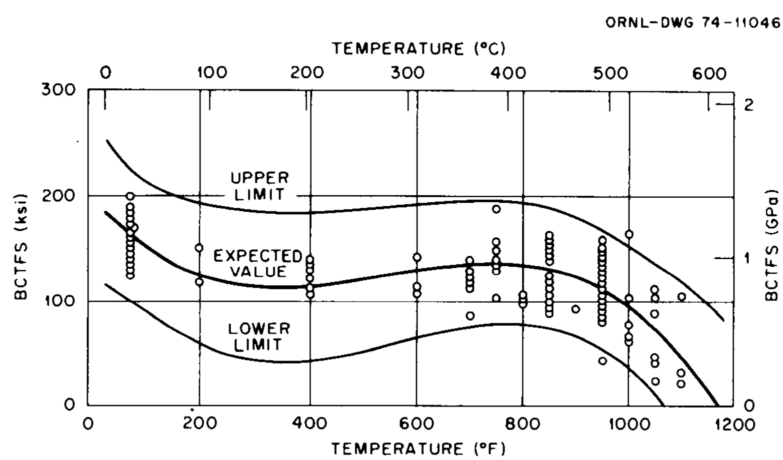

Fig. 4. Bridgman-Corrected True Fracture Stress vs Temperature, Including a Mean Regression Curve and Upper and Lower Tolerance Limits (P = 0.90, λ = 0.95).

specify with a confidence level of 0.95 the bounds within which 90% of the observed values are expected to fall. Each limit may be interpreted separately to mean that at this confidence level 95% of the observations are expected to fall above the lower limit, while 95% are also expected to fall below the upper limit. These tolerance limits are simultaneous in all levels of the independent variables; that is, they may be simultaneously calculated for different values of the independent variables without affecting the level of confidence. Calculation of tolerance limits is discussed in greater detail by Leiberman and Miller.[20]

The expected values of each of the above quantities [for stresses in MPa and temperatures (T) in °C] are given by

$$\mathrm{PL} = 151.26 - 0.1015T \ , \tag{1}$$

$$\mathrm{YS} = 263 - 0.315T + (9.39 \times 10^{-4})T^2 - (1.08 \times 10^{-6})T^3 \ , \tag{2}$$

$$\mathrm{UTS} = 527 - 1.03T + (4.54 \times 10^{-3})T^2 - (5.83 \times 10^{-6})T^3 \ , \tag{3}$$

$$\mathrm{TFS} = 1270 - 6.53T + 0.0266T^2 - (3.09 \times 10^{-5})T^3 \ . \tag{4}$$

The yield strength (447 data) and ultimate tensile strength (449 data) are the most frequently reported strength properties. The plots of these data in Figs. 1 and 2 show a considerable amount of scatter; presumably this scatter is due to variations in strain rate, chemistry, microstructure, and thermomechanical processing history. Smith[3,21,22] has presented a method for normalizing such data by taking the ratio of an elevated-temperature strength property to the corresponding strength measured at room temperature for each lot of material. A "trend" curve of strength ratio as a function of temperature is then derived, preferably by least-squares methods.

However, a major goal of the current program was to perform a statistical analysis of property variations, and the number and diversity of the available data made direct statistical treatment possible. Also, the data given here were generated over a wide range of nominal strain rates (10^{-4} – 10^{-1}/min); while these strain rate variations contribute to the scatter in the data, they cannot be "reduced" by the ratio

---

[20] G. T. Leiberman and R. G. Miller, Jr., "Simultaneous Tolerance Intervals in Regression," *Biometrika* 50: 165 (1963).

[21] G. V. Smith, "Evaluation of Elevated-Temperature Strength Data," *J. Mater.* 4: 878–908 (1969).

[22] G. V. Smith, "The Strength of 2 1/4 Cr-1 Mo Steel at Elevated Temperatures," pp. 1–26 in *Symposium on 2 1/4 Chrome 1 Molybdenum Steel in Pressure Vessels and Piping,* ed. A. O. Schaefer, ASME, New York, 1971.

technique, since the strain rate dependence is different at different temperatures. It should be noted that the room-temperature minima on yield strength and ultimate tensile strength obtained from the lower tolerance limits were 192 and 405 MPa (28 and 59 ksi), respectively, compared with the specified minima of 207 and 414 MPa (30 and 60 ksi) given above. This small difference is cause by the fact that all of the data considered influence the position of the tolerance limits at any temperatures, not just the data at room temperature.

Figure 3 shows the results of the analysis of proportional limit data (184 data points). These data were all obtained from tensile tests monitored using ASTM Class B-2 extensometers and electronic recording equipment,[23] which may have not been accurate enough to provide a good measure of the proportional limit in all cases. In this case, proportional limit was described merely as a linear function of temperature, whereas the other strength criteria were expressed as cubic functions of temperature. Higher order polynomial models for proportional limit were tried, but did not yield significantly better results than the linear model.

Another tensile property which has found some use (e.g., in predicting fatigue behavior[24]) is the true fracture stress, defined by the load at fracture divided by the cross-sectional area at fracture. Here, the area at fracture was calculated from post-test measurement of specimen diameter, and did not account for area reduction due to cracking and voidage within the specimen. The data were corrected for the effects of stress triaxiality developed during necking, using the Bridgmen correction factor[25] as calculated by the method of Nunes.[26] Figure 4 shows the results of the analysis of Bridgman-corrected true fracture stress (146 data points).

Ductility Properties

A limited investigation of the tensile ductility of 2 1/4 Cr-1 Mo steel has also been carried out. Properties studied include uniform elongation, total elongation, and reduction in area. All ductility values were expressed in percent strain.

Total elongation data came from tests involving specimens with gage lengths of approximately 50 mm, while the other two quantities should

---

[23]"Standard Method of Verification and Classification of Extensometers," ASTM Standard E83-67, Part 31, pp. 359–64 in *Annual Book of ASTM Standards*, ASTM, Philadelphia, 1973.

[24]S. S. Manson, "Fatigue: A Complex Subject – Some Simple Approximations," *Exp. Mech.* 193–226 (1965).

[25]P. W. Bridgman, "The Stress Distribution at the Neck of a Tension Specimen," *Trans. Am. Soc. Met.* 32: 553–74 (1944).

[26]J. Nunes, "Flow-Stress-Strain Relationships in Tensile Tests of Steel," *Mater. Res. Stand.* 3: 712–22 (1963).

be relatively insensitive to gage length variations for specimens having a ratio of gage length to diameter of 4:1 or greater. Figures 5–7 show the results of the analyses for each of these quantities.

Strain Rate and Strain Aging Effects

The above tensile properties are also functions of factors other than temperature (chemical composition, metallurgical structure, strain rate, etc.). Evaluation of the effects of such factors is difficult and complex. However, the intent here was to determine general trends, and therefore it was deemed acceptable to express the models in terms of temperature only. Certain qualitative insights can be gained, however, from a further look at the data. Note that all strength properties except proportional limit exhibit maxima or inflections in the temperature region 300 to 450°C. Moreover, the ductility properties exhibit minima roughly in the same region.

Analysis of the strain rate effects on the properties of a single lot of annealed 2 1/4 Cr-1 Mo steel revealed that at low temperatures the effects were negligible.[27] In the region 300 to 450°C, however, lower strain rates tend to yield higher strength and lower ductility. These effects indicate the occurrence of dynamic strain aging.[28] At temperatures above 450°C, lower strain rates tend to yield lower strength, as expected.[27,29]

CREEP PROPERTIES

Since 2 1/4 Cr-1 Mo steel is often used at service temperatures up to 600°C in nonnuclear applications, successful design requires the consideration of creep properties. Indeed, creep may need to be considered when the alloy is used at temperatures above about 375°C. Therefore, the constant-load, uniaxial creep properties in the region 375 to 600°C were studied in some detail.

---

[27] R. L. Klueh and T. L. Hebble, *A Mathematical Description for the Stress-Strain Behavior of Annealed 2 1/4 Cr-1 Mo Steel,* ORNL-TM-4928 (June 1975).

[28] J. D. Baird, "Strain Aging of Steel — A Critical Review — Part III, Dynamic Strain Aging," *Iron Steel* 450–57 (1963).

[29] C. R. Brinkman, R. K. Williams, R. L. Klueh, and T. L. Hebble, "Mechanical and Physical Properties of 2 1/4 Cr-1 Mo Steel in Support of CRBRP," presented at International Conference on Materials for Nuclear Steam Generators, Gatlinburg, Tenn., Sept. 9–12, 1975.

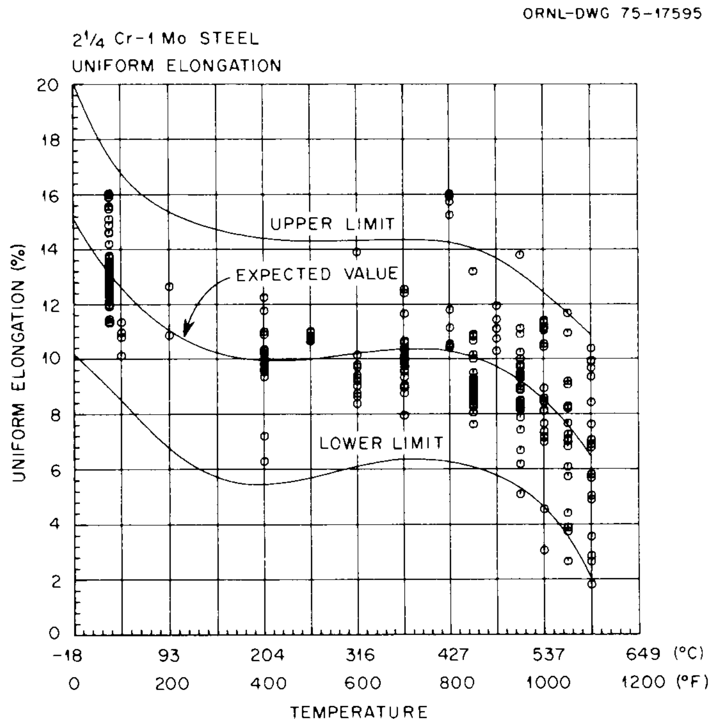

Fig. 5. Uniform Elongation vs Temperature, Including a Mean Regression Curve and Upper and Lower Tolerance Limits (P = 0.90, λ = 0.95).

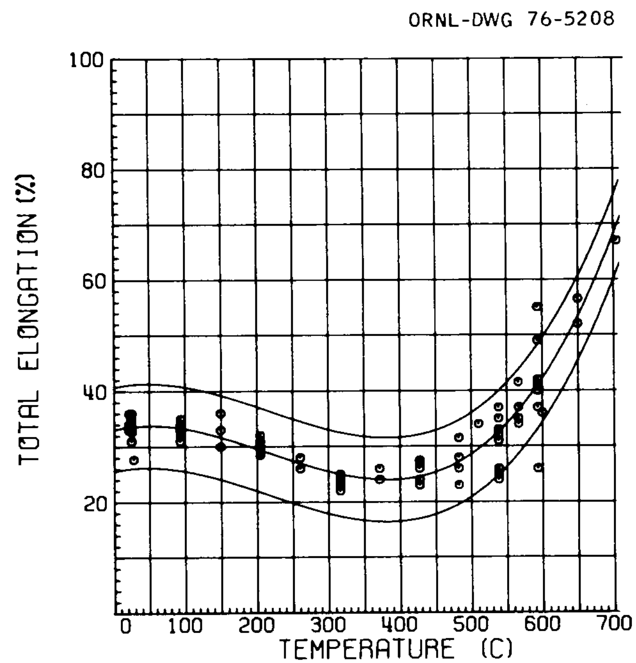

Fig. 6. Total Elongation in 50 mm vs Temperature, Including a Mean Regression Curve and Upper and Lower Tolerance Limits (P = 0.90, λ = 0.95).

ORNL-DWG 76-5209

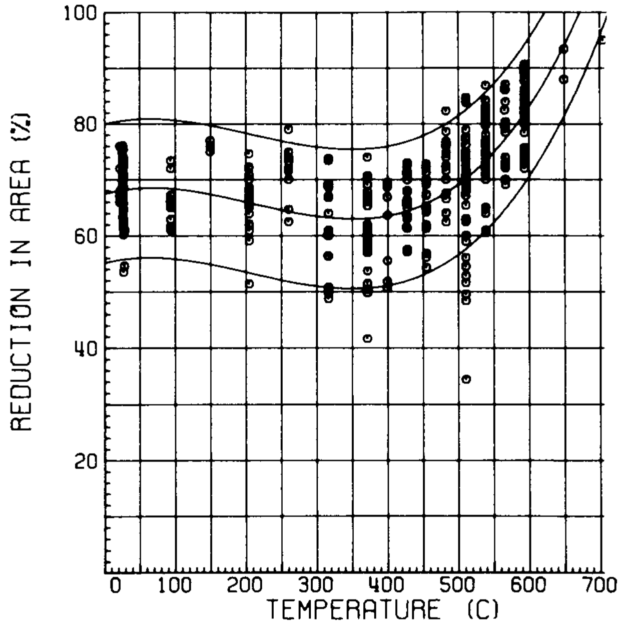

Fig. 7. Reduction in Area vs Temperature, Including a Mean Regression Curve and Upper and Lower Tolerance Limits (P = 0.90, λ = 0.95).

Creep Equation

As a first and important step, available isothermal strain-time creep curves were collected in order to formulate a model for creep strain as a function of time, temperature, and engineering stress. Since a single equation can describe only a consistent set of curves, analysis was limited to curves displaying classical initial primary creep behavior. Unfortunately, however, only a few such curves with precise strain measurements were obtainable for annealed material.

Also, since room-temperature ultimate tensile strength was found to have a significant effect on the deformation behavior, only tests on material with room-temperature ultimate tensile strength in the range 490—520 MPa (71—75 ksi) (approximately average) were used in order to reduce the number of variables in the initial analysis. The final data set used consisted of three multitest sets of creep curves from references 10, 11, and 13 containing a total of 37 tests with creep times reaching 5000 hr. The tests were conducted at temperatures ranging from 454 to 593°C. Many other tests were omitted because the curves were concave upward throughout the test, displaying no classical primary creep. Such behavior was commonly associated with high stresses and may have been caused in part by effects incurred during loading. Fortunately, design applications will be mainly concerned with lower stress levels.

Once the data base of 37 tests had been established, the next step was to select an analytical model that could adequately describe the strain-time behavior of each individual curve. After consideration of and analysis by several standard forms of creep equations,[30] a model of the following form was selected:

$$e_c = \frac{t}{A + Bt} + \dot{e}_m t , \tag{5}$$

where e_c = engineering creep strain, t = creep time, $\dot{e}_m$ = minimum creep rate (%/hr), and A and B are functions of stress and temperature.

This model consists of a transient primary creep term and a linear secondary creep term, the form being identical to that proposed by Oding.[31] The total contribution of the primary term tends toward $1/B$ as t becomes large, so that $1/B$ might be called the "transient creep strain." Meanwhile, $1/A$ is the initial slope of the primary term. Depending on the values of A and B, this equation can produce a long-arching curve, or a sharply bending curve.

Having fit Eq. (5) to all of the 37 available creep curves by means of nonlinear least-squares analysis, the next step was to express the coefficients A, B, and $\dot{e}_m$ as functions of stress (σ) and temperature (T). After investigation of various equation forms, the following models were chosen for these functions (for T in °R and σ in ksi):

$$\log_{10} A = 12.26 - 3.348 \times 10^{-6}T^2 + 9.353 \times 10^{-4}\sigma^2 - 1.167 \times 10^{-4}T\sigma , \tag{6}$$

$$\log_{10} B = -52.19 + 8.682 \times 10^{-2}T - 3.308 \times 10^{-5}T^2 - 1.152(\log_{10} \sigma)^2 , \tag{7}$$

$$\log_{10} \dot{e}_m = -30.04 + 1.516 \times 10^{-2}T + 2.001 \times 10^{-3}T(\log_{10} \sigma)^2 . \tag{8}$$

These relationships provide a reasonable description of the values obtained from the individual curve fits, although the scatter is large, especially in A and B. Figure 8 shows the results of the fit to the A values. The equations for A and $\dot{e}_m$ are mathematically valid at least from 375 to 600°C, although use below 454°C represents extrapolation in temperature and should be done with caution. On the other hand, the second-order temperature term in the model for B [Eq. (7)] causes a minimum in the plot of B vs T at approximately 440°C. Therefore it is recommended that, at temperatures below 440°C, the value of B calculated at 440°C be used. Also, Eqs. (7) and (8) exhibit minima as functions of stress at σ = 7 MPa (1 ksi) ($\log \sigma_{ksi} = 0$), which is clearly unrealistic. Equation (6), meanwhile, produces unreasonable results at values of σ greater than about

---

[30] J. B. Conway, *Numerical Methods for Creep and Rupture Analyses*, Gordon and Breach, New York, 1968.

[31] I. A. Oding, ed., *Creep and Stress Relaxation in Metals* (translated by E. Bishop; English editor, A. J. Kennedy), Oliver and Boyd, London, 1959, pp. 78–82.

ORNL-DWG 76-5908

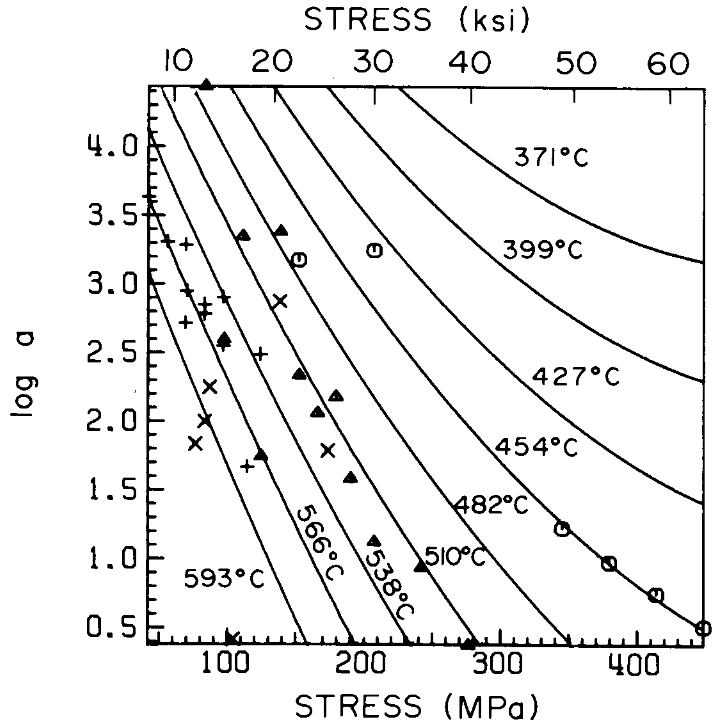

Fig. 8. The *A* Parameter Eq. (5) vs Stress at Various Temperatures. Points Represent Least-Squares Fits of Eq. (5) to Individual Creep Curves; Lines Calculated from Eq. (6).

450 MPa (65 ksi). Thus, Eq. (5) is mathematically valid for temperatures from 375 to 600°C and for stresses from 7 to 450 MPa (1 to 65 ksi). The upper limit in time on the equation is the time to the onset of tertiary creep, discussed below.

The use of Eq. (5) to describe creep behavior has several advantages, including the above-noted flexibility and the fact that all of the constants in the equation have a clear physical interpretation in terms of the actual creep curve. An additional advantage is the fact that Eq. (5) may be solved for time as a function of strain, allowing use of the equation in strain-hardening type of analyses of variable-loading creep behavior and for description of relaxation behavior. A simple algebraic manipulation of Eq. (5) yields

$$t = \frac{be - a\dot{\varepsilon}_m - 1 \pm \sqrt{(a\dot{\varepsilon}_m + 1 - be)^2 + 4aeb\dot{\varepsilon}_m}}{2b\dot{\varepsilon}_m} \quad . \tag{9}$$

This equation, of course, yields two values for time at a given strain, but the value involving the negative square root is always negative, leaving only one positive time value. Reference 32 describes prediction

[32] J. B. Conway, R. H. Stentz, and J. T. Berling, *Fatigue, Tensile, and Relaxation Behavior of Stainless Steels*, USAEC Report TID-26135.

of relaxation behavior based on creep behavior. Figure 9 illustrates results obtained by using Eq. (9) in conjunction with strain-hardening assumptions. The agreement with actual experimental relaxation data is good; however, the amount of relaxation data available is limited.

Equation (5) was derived from data for 37 tests on 3 lots of material covering a limited range of room-temperature strengths. The obvious question that arises is whether or not the equation describes the behavior of annealed 2 1/4 Cr-1 Mo steel in general. Clearly it does not apply to those tests involving no primary creep. Otherwise, this question is dealt with below.

First, a large number of creep curves were available, although most of these were either of nonclassical form, were obtained by somewhat imprecise strain measuring techniques (e.g., measurements obtained from load train motion rather than from direct extensometer measurements), or were for material outside the above specified strength range. These curves could not be used in the development of Eqs. (6), (7), and (8), but the comparison of the predictions of the creep equation with actual data provides a measure of the applicability of the equation. A total of 192 curves (including the 37 used above) were available from refs. 4, 10, 11, and 13 at temperatures from 454 to 677°C. These data have been analyzed by plotting stress against the time to a given percent strain on log-log plots, thus obtaining data presentation analogous to stress-rupture isothermals. Data for time to 0.1, 0.25, 0.5, 1.0, 1.5, 2.0, and 3.0% creep strain have been examined. For comparison with the creep equation results, these data have also been directly analyzed by means of several models. Figures 10 and 11 illustrate comparisons between such data and predictions from the creep equation. Clearly, the predictions of Eq. (5) agree well with the data, although the data exhibit considerable scatter.

A possible generalization of the creep equation could be obtained by replacing Eq. (8) with an equation determined by analysis of all available data for minimum creep rate. Analysis of minimum creep rate data shows that adequate correlation can be obtained by a model of the form

$$\log \dot{e}_m = 1.979 + 6.961 \times 10^{-5}\tau T - 0.097\tau + 0.01459\tau \log \sigma \ , \qquad (10)$$

where T is the temperature (K), σ the stress (MPa), and τ the room-temperature ultimate tensile strength (MPa) of the lot of material under consideration. Equation (10) is valid from 371 to 593°C (700 to 1100°F) over a stress range of 1 MPa to τ, for values of $\dot{e}_m \geq 10^{-6}$ %/hr. Figure 12 compares the predictions of Eqs. (8) and (10) with actual data at 538 and 593°C. The two equations agree reasonably well. Substitution of Eq. (10) for Eq. (8) in the creep equation yields the results shown by the filled triangles in Figs. 10 and 11. In Figs. 10–12 an average τ value of 507 MPa (73.6 ksi) from Eq. (3) has been used, while Fig. 12 also includes calculations using a minimum value[33] of 414 MPa (60 ksi).

---

[33] *Interpretations of the ASME Boiler and Pressure Vessel Code, Code Case 1592*, ASME, New York, 1974.

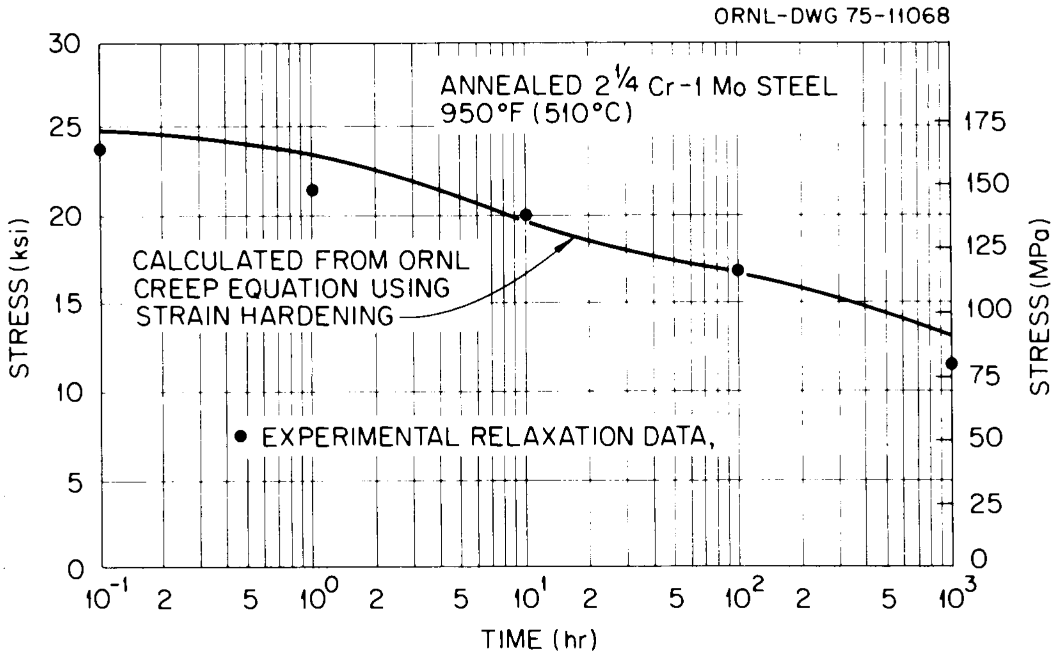

Fig. 9. Comparison of a Relaxation Curve Calculated from Eq. (9) with Actual Experimental Relaxation Data at 510°C.

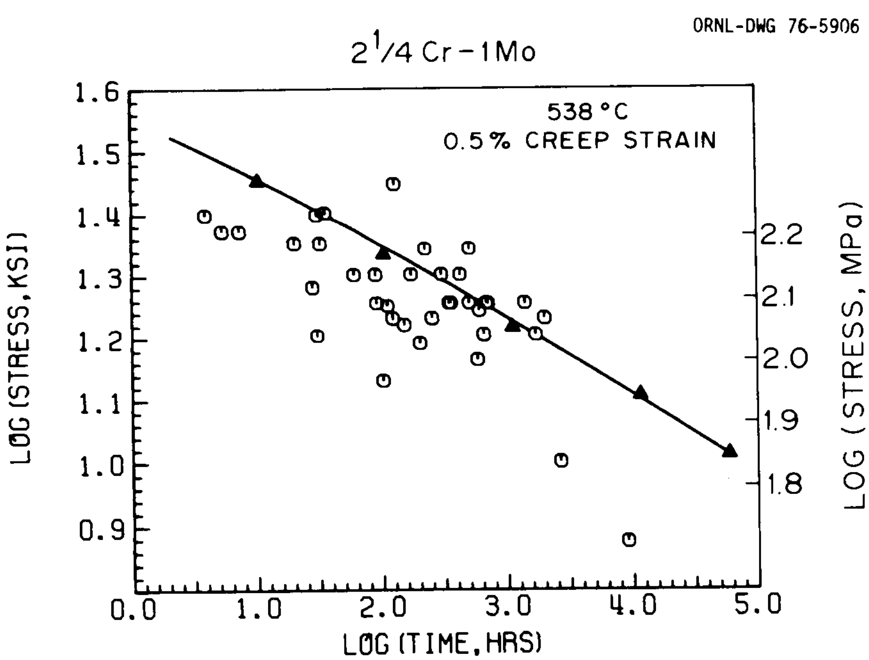

Fig. 10. Data for Time to 0.5% Creep Strain at 538°C. Lines calculated from creep equation; open points represent experimental data; filled points represent predictions from the creep equation, using Eq. (10) for minimum creep rate.

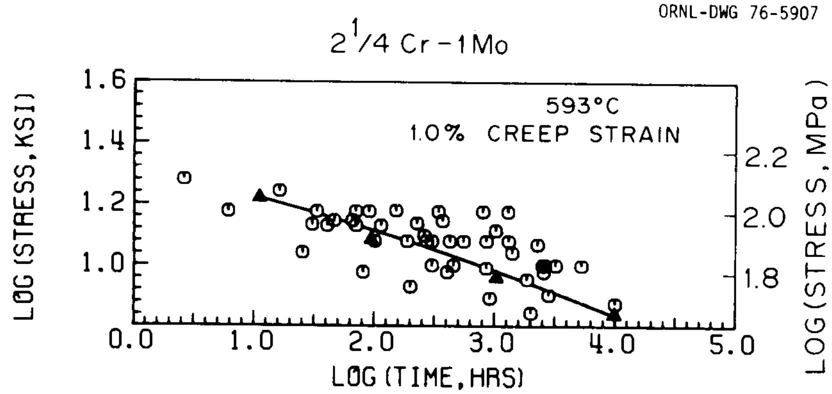

Fig. 11. Data for Time to 1.0% Creep Strain at 593°C. Lines calculated from creep equation; open points represent experimental data; filled points represent predictions from the creep equation, using Eq. (10) for minimum creep rate.

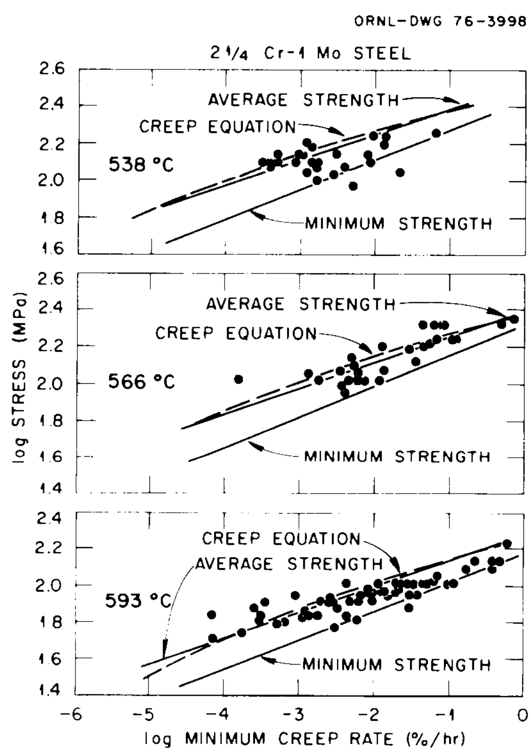

Fig. 12. Minimum Creep Rate vs Stress at Various Temperatures. Solid lines calculated from Eq. (10); dashed lines calculated from Eq. (8).

Clearly, for average strength material, use of Eqs. (8) and (10) yields nearly equivalent results. For use of the creep equation over wider ranges of material strength, Eq. (10) might be used to predict minimum creep rate, although this procedure yields no estimate of possible variations in the primary creep behavior with τ.

Finally, Fig. 13 compares isochronous stress-strain curves calculated from Eq. (5) with those appearing in ASME Code Case 1592.[33] These curves include total strain—creep strain plus instantaneous strain incurred upon loading. In the curves calculated from the creep equation, the instantaneous strains were obtained from monotonic tensile stress-strain curves in the code case[33] at this temperature. The agreement is quite good.

A complete discussion of the derivation, use, and possible generalization of the current creep equation will be presented elsewhere.[34] The current comparisons, however, indicate that based on the available data the equation represents the creep behavior of annealed 2 1/4 Cr-1 Mo steel.

Time to Tertiary Creep

Clearly, the above creep equation is not valid beyond the onset of tertiary creep. Moreover, current U.S. design rules[33] include the stress to cause onset of tertiary creep as one of the criteria to be considered in elevated-temperature situations. Therefore, it is useful to be able to express the expected time to tertiary creep as a function of stress and temperature. To accomplish the goal, a total of 97 tests with temperatures ranging from 454 to 593°C were analyzed. These tests involved measurement of the 0.2% offset time to tertiary creep.[35]

Data for time to tertiary creep have been successfully analyzed[35] using standard time-temperature parameters that were developed for the treatment of rupture life data. In the current analysis, these parameters, a specialized form of the minimum committment method,[36] and a wide variety of algebraic models have been tried. However, due to the relatively limited range of the available data and the fairly large amount of scatter, direct analysis raises problems. In particular, the lower tolerance limits are unreasonably conservative at long times, for example, 10^5 hr. Alternatively, as described in ref. 35, the expected

---

[34] M. K. Booker, D. O. Hobson, and T. L. Hebble, *Creep Strain-Time Characteristics of Annealed and Isothermally Annealed 2 1/4 Cr-1 Mo Steel*, report in preparation.

[35] M. K. Booker and V. K. Sikka, "Interrelationships Between Creep Life Criteria for Four Nuclear Structural Materials," *Trans. Am. Nucl. Soc.* 21: 155–56 (1975).

[36] S. S. Manson and C. R. Ensign, *A Specialized Model for Analysis of Creep-Rupture Data by the Minimum Committment, Station Function Approach*, NASA-TM-S-52999 (1970).

ORNL-DWG 75-9494

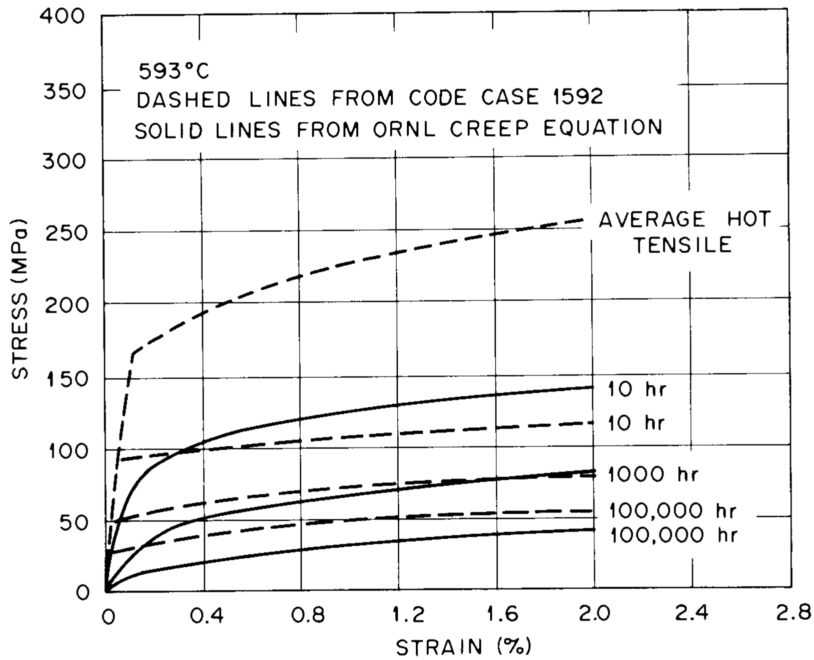

Fig. 13. Comparison of Average Isochronous Stress-Strain Curves in Code Case 1592 with Curves Generated from Eq. (5) at 593°C.

time to tertiary creep, t_3 (hr), can be well described as a function of rupture life, t_r (hr) by

$$t_3 = 0.28 t_r^{1.07} , \qquad (11)$$

as shown in Fig. 14. Rupture life is given as a function of stress and temperature in the next section, which allows an expression of t_3 as a function of stress and temperature. Lower limits on t_3 as a function of stress and temperature may be calculated as follows. First, determine $G(\sigma,T)$ = lower limit on t_r in σ and T by the use of tolerance limits. Next, determine $F(t_r)$ as the lower tolerance limit on Eq. (11) as shown in Fig. 14. Then the lower limit on $t_3(\sigma,T)$ is given by $F[G(\sigma,T)]$. Calculated values and lower limits for t_3 are compared with data in Fig. 15. Previous investigators have found t_3 to be about $0.4t_r$ in one case[37] and about $0.25t_r$ in another[38] for this material.

---

[37]R. Viswanathan, "Strength and Ductility of 2 1/4 Cr-1 Mo Steels in Creep at Elevated Temperatures," *Met. Tech.* 1: 284–94 (1974).

[38]J. E. Bynum, F. V. Ellis, and B. W. Roberts, "Creep and Tensile Properties and Constitutive Equations for a 2 1/4 Cr-1 Mo Steel," *Structural Materials for Service at Elevated Temperatures*, ASME, New York, 1975, pp. 146–66.

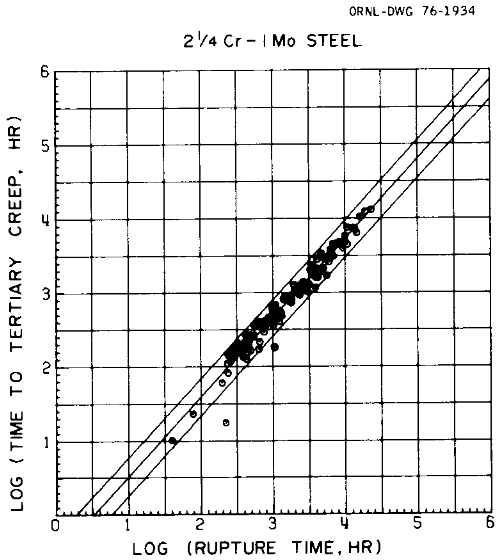

Fig. 14. Relationship Between Rupture Life and Time to the Onset of Tertiary Creep.

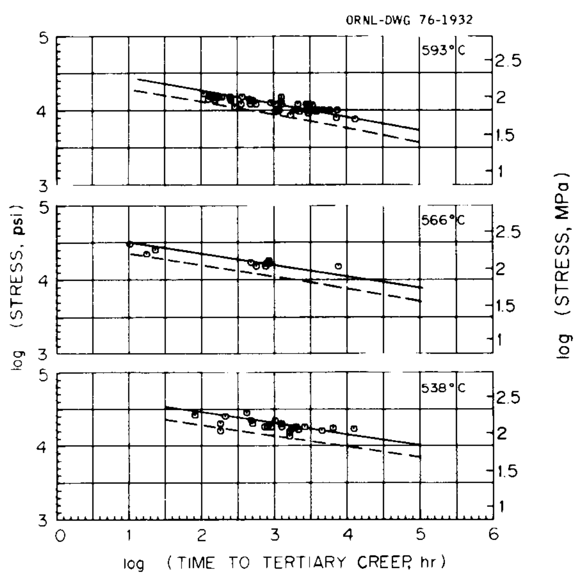

Fig. 15. Time to Tertiary Creep vs Stress at Various Temperatures, Including Predicted Isothermals and Lower Limits from Eq. (11).

The use of Eq. (11) to provide an upper limit on the applicability of the creep equation involves two complications: (1) the value of t_3 in Eq. (11) is an offset value and is therefore slightly larger than the true limit on the applicability of Eq. (5); and (2) Eq. (11) was derived from a somewhat different data base, including some concave upward nonclassical creep curves. Nevertheless, it is felt that t_3 as given in Eq. (11) is the best available limit. The equation is valid from 371 to 593°C (700 to 1100°F) at stresses greater than 1 MPa (0.15 ksi) and less than 450 MPa (65 ksi) for t_3 up to 10^5 hr.

It should be noted that lower limits on stress to cause onset of tertiary creep calculated from Eq. (11) fall slightly below the S_{mt} values given in ref. 17 at long times ($t_3 \geqslant 10^4$ hr) when reduced by the appropriate safety factor (0.8). However, the lower limits given here are not necessarily intended for the calculation of design-allowable stress levels.

Rupture Life

The creep property that has received the most attention in the literature, and for which the most data are available, is rupture life. In particular, design codes[39,40] include criteria based on stress-rupture behavior. Thus, it was desirable to obtain an equation expressing rupture life as a function of stress and temperature.

The rupture life data bases used consisted of the results from 563 tests conducted at temperatures ranging from 454 to 600°C. These tests were conducted at stresses ranging from 34 to 345 MPa (5 to 50 ksi), with rupture lives reaching 50,000 hr. As with the other creep properties, data at temperatures above 600°C were omitted, while data at temperatures below 454°C were not available. The omission of the higher temperature data is contrary to a usual time-temperature parametric analysis. However, in this case analysis of data up to 677°C showed that the higher-temperature data displayed different behavior than the data used. This difference could have been due to the effects of oxidation or to a change in fracture mode from transgranular to intergranular.

The data were analyzed by a statistical evaluation of a list of candidate algebraic models, which included many standard time-temperature parameters as a subset. Briefly, the method consists in first specifying possible terms (σ, $\log \sigma$, T, $1/T$, $T \log \sigma$, $1/T \log \sigma$, etc.) that might appear in a model and then evaluating all models that can be formed from subsets of these terms. The procedure is described in detail in ref. 41.

The final model chosen to represent rupture life was of the form

$$\log t_r = -31.45 + \frac{3.932 \times 10^4}{T} - 19.75 \log \sigma + 0.01642 T \log \sigma \;, \quad (12)$$

---

[39] *1974 ASME Boiler and Pressure Vessel Code, Section III, Nuclear Power Plant Components*, ASME, New York, 1974.

[40] *Interpretations of the ASME Boiler and Pressure Vessel Code, Code Case 1592*, ASME, New York, 1974.

[41] M. K. Booker, *Mathematical Description of the Elevated-Temperature Creep Behavior of Type 304 Stainless Steel* (report in preparation).

where

t_r = rupture life (hr),

T = temperature (K),

σ = stress (MPa).

Equation (12), being linear in log σ vs t_r, should be extrapolated with caution, since there are some indications of downward curvature at long times in the higher temperature log σ vs log t_r isotherms ($T > 566°C$, $t_r >$ 2×10^4 hr). This equation is mathematically valid from 371 to 593°C (700 to 1100°F) at stresses greater than 1 MPa (0.15 ksi) and less than 450 MPa (65 ksi), for times up to 3×10^5 hr. Stress-rupture isothermals calculated from this model are shown in Fig. 16 for various temperatures, including upper and lower tolerance limits. The fit of the data is quite good, although there is a fairly large amount of scatter. The isothermals form straight lines in log-log plots of stress vs rupture life. Although, by convention, Figs. 15 and 16 are plotted in terms of log σ vs log t_r, it must be realized that time is the dependent and σ the independent variable and that the actual analysis was conducted accordingly. For instance, the tolerance limits apply to time at a given stress, not vice versa. Table 1 compares lower-limit values of rupture strength calculated from

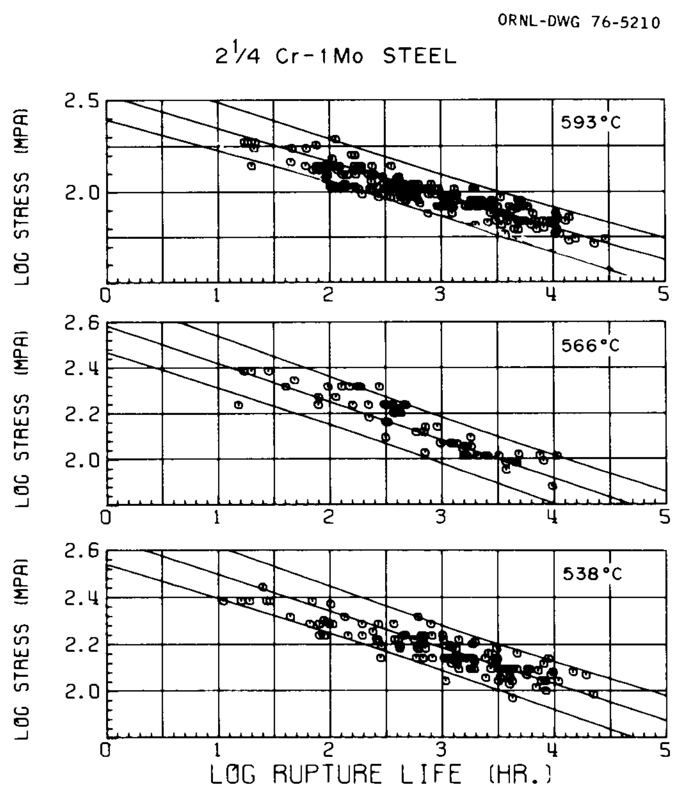

Fig. 16. Time to Rupture vs Stress at Various Temperatures, Including Mean Lines and Upper and Lower Tolerance Limits (P = 0.90, λ = 0.95) Calculated from Eq. (12).

Table 1. Comparison of Current Lower-Limit Stress-to-Rupture Values With Minimum Stress-to-Rupture Values in ASME Code Case 1592

Temperature [°C (°F)]	Rupture Time (hr)	Current Investigation Rupture Stress (MPa)	ASME Code Case 1592 Rupture Stress (MPa)
427 (800)	10^3	338	296
	10^4	254	238
	10^5	181	186
482 (900)	10^3	203	193
	10^4	144	149
	10^5	99	113
538 (1000)	10^3	125	123
	10^4	91	90
	10^5	56	65
593 (1100)	10^3	74	74
	10^4	48	52
	10^5	30	34

Eq. (12) and taken from refs. 17 and 42. The slight variations seen among the present results and those in refs. 17 and 42 are due to differences in data bases and differences in analytical techniques. Again, however, the values given here are not necessarily intended for the calculation of allowable stresses.

Creep Ductility

Values of rupture elongation and reduction in area in creep show too much scatter to permit direct analysis. Some indirect estimates of creep ductility can be made, however. For instance, the strain predicted by Eq. (5) at a time equal to the corresponding time to tertiary creep from Eq. (11) provides an estimate of the creep strain to tertiary creep. Indirect parametric and empirical methods for the analysis of creep ductility data are given in refs. 42, 43, 44, and 45, including some results for 2 1/4 Cr-1 Mo steel.

---

[42]G. V. Smith, *Supplemental Report on the Elevated-Temperature Properties of Chromium-Molybdenum Steel (an Evaluation of 2 1/4 Cr-1 Mo Steel)*, *ASTM Data Ser. Publ.* DS-6-S2, ASTM, Philadelphia, 1971.

[43]M. K. Booker, C. R. Brinkman, and V. K. Sikka, "Correlation and Extrapolation of Creep Ductility Data for Four Elevated-Temperature Structural Materials," *Structural Materials for Elevated-Temperature Nuclear Power Generation Service*, ASME, New York, 1975, pp. 108–45.

[44]M. K. Booker and V. K. Sikka, "Predicting the Strain to Tertiary Creep for Four Structural Materials," presented at the 1975 Winter Meeting of the American Nuclear Society, San Francisco, Calif., Nov. 16–21, 1975, report in preparation.

[45]M. K. Booker and V. K. Sikka, *Empirical Relationships Among Creep Properties of Four Elevated-Temperature Structural Materials*, report in preparation.

FATIGUE PROPERTIES

The fully reversed, strain-controlled, continuous-cycling fatigue properties of annealed and isothermally annealed 2 1/4 Cr-1 Mo steel have been reported in some detail.[46,47] Average best-fit curves of strain range vs cycles to failure at various temperatures are shown in Fig. 17. In constructing these curves, some load-controlled data were used in regions of very high-cyclic life (where behavior is essentially elastic) with values of load range converted to strain range, using Young's modulus. The curves were obtained from least-squares fits to data at the temperatures of applicability. It should be noted that the temperature dependence below 427°C (800°F) can be complicated. For instance, the data taken at 316°C show about the same low-cycle fatigue lives as do the room-temperature data. In the high-cycle region, however, the 316°C data exhibit fatigue lives well exceeding those at room temperature, possibly again due to strain aging effects. These curves are valid for strain rates $\geqslant 4 \times 10^{-3}$ sec^{-1} and do not account for the effects of mean stress or strain. The equations for these curves are as follows:

427°C (800°F)

$$\log N_f = 3.578 - 2.358 \log \Delta\varepsilon_t + 3.506(\log \Delta\varepsilon_t)^2 - 4.197(\log \Delta\varepsilon_t)^3 , \quad (13)$$

538°C (1000°F)

$$\log N_f = 3.302 - 2.388 \log \Delta\varepsilon_t + 3.521(\log \Delta\varepsilon_t)^2 - 2.577(\log \Delta\varepsilon_t)^3 , \quad (14)$$

593°C (1100°F)

$$\log N_f = 3.153 - 1.803 \log \Delta\varepsilon_t + 2.613(\log \Delta\varepsilon_t)^2 - 3.738(\log \Delta\varepsilon_t)^3 , \quad (15)$$

where

N_f = cycles to failure,
$\Delta\varepsilon_t$ = total strain range (%).

---

[46] C. R. Brinkman, M. K. Booker, J. P. Strizak, and W. R. Corwin, "Elevated-Temperature Fatigue Behavior of 2 1/4 Cr-1 Mo Steel," *Trans. ASME* 97 (4): Ser. J., 252–57 (1975).

[47] C. R. Brinkman, M. K. Booker, J. P. Strizak, W. R. Corwin, J. L. Frazier, and J. M. Leitnaker, *Interim Report on the Continuous-Cycling Elevated-Temperature Fatigue and Subcritical Crack Growth Behavior of 2 1/4 Cr-1 Mo Steel,* ORNL-TM-4993 (December 1975).

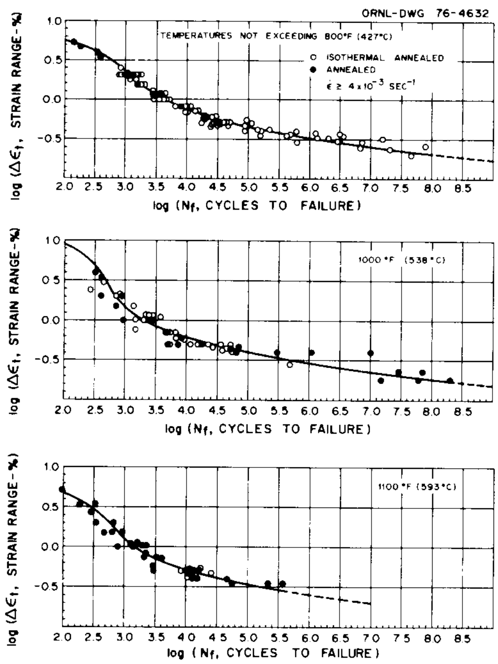

Fig. 17. Average Fatigue Life Curves from Room Temperature to 593°C, Including Raw Data.

Equations (13) and (14) may be used from 10^2 to 2×10^9 cycles, Eq. (15) from 10^2 to 2×10^7 cycles. Slight extrapolation is possible, since these polynomials undergo no extrema or inflections in the high-cycle range. The temperatures shown are the maximum temperatures of applicability of the given equations.

The data show a relatively small dependence of cyclic life on temperature at a strain rate of 4×10^{-3} sec^{-1}. However, recent tests at ORNL and elsewhere[48,49] have shown that the fatigue life of this material depends on strain rate at temperatures as low as 370°C, because of strain aging, and at higher temperatures because of creep effects (creep-fatigue-environment interaction).

An extensive evaluation of the creep-fatigue behavior of 2 1/4 Cr-1 Mo steel will be made when current programs of data generation are completed. Results obtained thus far indicate several trends: (1) compression hold times are somewhat more damaging than tensile holds; (2) hold time effects are greater at low strain ranges than at higher strain ranges; (3) at a given temperature and strain rate, imposition of hold times results in an increase in the plastic strain range and a decrease in total stress range.

---

[48] H. G. Edmunds and D. J. White, "Observations of the Effect of Creep Relaxation on High-Strain Fatigue," *J. Mech. Eng. Sci.* 8: 310–21 (1966).

[49] S. S. Manson, G. R. Halford, and M. H. Hirschberg, *Creep-Fatigue Analysis by Strain-Range Partitioning,* NASA-TM-X-67838 (1971).

IMPACT PROPERTIES

The variation of Charpy V-notch impact energy with temperature gives an indication of trends toward brittle behavior in a material, and thus can be a useful design consideration when the possibility of brittle fracture exists. For 2 1/4 Cr-1 Mo steel in the annealed or isothermally annealed condition, this variation was found to be describable by a model of the form

$$E = A\{1 - \exp[-B(T - C)^2]\} \ , \quad (16)$$

valid at $T > C$, where

E = energy absorbed at fracture (J),

T = temperature (°C),

A, B, C = empirical constants.

In this model, the predicted energy is zero at temperature equal to C, rises sigmoidally, and levels off at an "upper-shelf" energy equal to A. However, lot-to-lot and heat treatment (cooling rate, etc.) variations are so great in the impact properties that it was necessary to estimate the constants in the above model for each separate combination of lot and heat treatment (nine combinations were considered). Values of A ranged from 82 to 227 J, B ranged from 2.2×10^{-5} to 6.29×10^{-4}, and C ranged from −90 to 4°C. Figure 18 illustrates the fit of Eq. (16) to one particular set of data for annealed plate (25 mm thick).

Note that, if one defines the ductile-brittle transition temperature (DBTT) as the temperature corresponding to a given energy, the DBTT can be estimated from the above model. Results of such estimations for an energy of 30 J, for instance, give a DBTT of −7 ± 11°C, while an energy of 10 J gives a DBTT of −23 ± 10°C for plate material.

CONCLUSIONS

A large collection of mechanical properties data for annealed and isothermally annealed 2 1/4 Cr-1 Mo steel has been used to develop analytical descriptions of the mechanical properties of this material. Specific conclusions are as follows:

1. The 0.2% yield strength, true fracture stress, and ultimate tensile strength can be adequately described by third-order polynomials in temperature. Corresponding central tolerance limits yield estimates of minimum and maximum expected strength. Peaks seen in these strength properties (especially ultimate tensile strength) in the range of 300 to 450°C indicate dynamic strain aging effects. Moreover, the proportional limit may be described as a linear function of temperature, since it

ORNL-DWG 76-5211

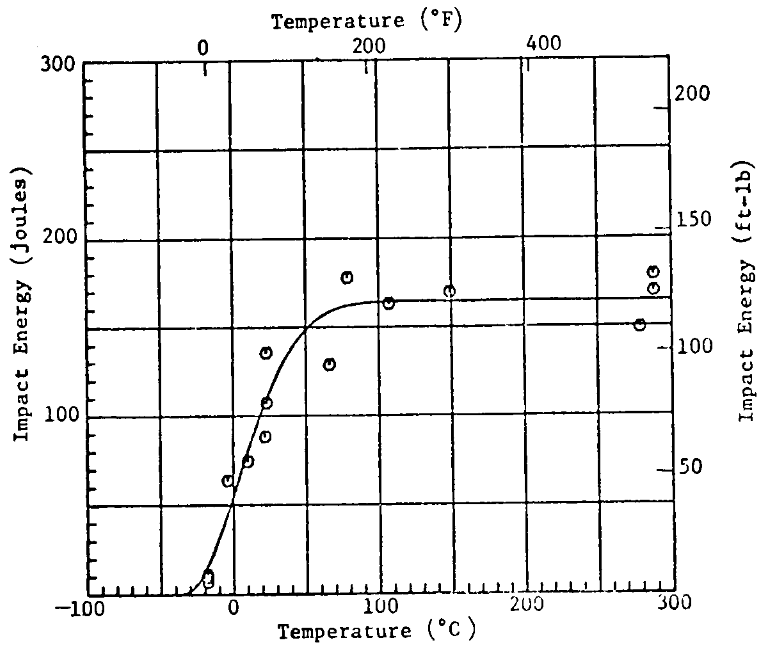

Fig. 18. Fit of Eq. (14) to Charpy V-Notch Impact Data for a Single Heat of Annealed Plate Material.

exhibits no peak. Lack of a peak in proportional limit is consistent with the above strain aging interpretation, since little dynamic strain aging can occur before the onset of measurable amount of plastic strain.

2. Short-term tensile ductility (uniform elongation, total elongation, and reduction in area) can also be described by third-order polynomials in temperature. Minima in the values of these properties in the range of 300 to 450°C again indicate strain aging effects.

3. A creep equation of the form $e_c = t/(A + Bt) + \dot{e}_m t$ was found to adequately describe creep strain as a function of stress, temperature, and time. While developed for only three lots of material, this equation appears to be consistent with the average behavior of 2 1/4 Cr-1 Mo steel in general.

4. Rupture life was described by mathematical models expressed as functions of temperature and stress, while minimum creep rate requires the inclusion of room-temperature ultimate tensile strength as an additional independent variable to achieve adequate correlation. Time to tertiary creep was described as a function of rupture life.

5. Strain- and load-controlled continuous-cycling fatigue data from recent test programs and from the literature were used to construct curves of strain range vs cycles to failure. Results for tests including hold times are still preliminary, but hold times at low strain ranges at temperatures greater than about 370°C are definitely detrimental to fatigue life, with compressive hold times being more damaging than tensile hold times.

6. A mathematical model describing Charpy V-notch impact energy as a function of test temperature was developed for single combinations of lot and heat treatment. This model allows estimates of the ductile-brittle transition temperature, although lot-to-lot and heat treatment variations are large.

ACKNOWLEDGMENTS

The authors gratefully acknowledge the contributions of those who have aided in these efforts. These contributors include all those who have supplied data (see references) for this effort, and E. Leach and C. K. Bayne, for aid in data analyses; V. K. Sikka, R. T. King, and W. R. Martin for reveiwing the manuscript; B. Parker for editing and Regina Collins for preparing the manuscript.

ORNL/TM-5329
UC-79b, -h, -k
(Liquid Metal Fast
Breeder Reactors)

INTERNAL DISTRIBUTION

1–2. Central Research Library
3. Document Reference Section
4–8. Laboratory Records Department
9. Laboratory Records, ORNL RC
10. ORNL Patent Office
11. G. M. Adamson, Jr.
12. S. E. Beall
13. R. G. Berggren
14–23. M. K. Booker
24. C. R. Brinkman
25. E. E. Bloom
26. D. A. Canonico
27. J. A. Conlin
28. J. M. Corum
29. W. R. Corwin
30. F. L. Culler
31. J. E. Cunningham
32. J. H. DeVan
33. D. P. Edmonds
34. W. R. Gall
35. G. M. Goodwin
36. R. J. Gray
37. W. L. Greenstreet
38. W. O. Harms
39. T. L. Hebble
40–42. M. R. Hill
43. J. P. Hammond
44. D. O. Hobson
45. F. J. Homan
46. H. Inouye
47. P. R. Kasten
48. J. F. King
49. R. T. King
50. R. L. Klueh
51. J. M. Leitnaker
52. A. L. Lotts
53. C. T. Liu
54. K. C. Liu
55. A. S. Lystrup
56. R. E. MacPherson
57. W. R. Martin
58. H. E. McCoy, Jr.
59. H. C. McCurdy
60. C. J. McHargue
61. R. K. Nanstad
62. H. Postma
63. P. Patriarca
64. C. E. Pugh
65. T. K. Roche
66. J. L. Scott
67. V. K. Sikka
68. G. M. Slaughter
69. W. J. Stelzman
70. J. O. Stiegler
71. J. P. Strizak
72. R. W. Swindeman
73. D. B. Trauger
74. W. E. Unger
75. T. N. Washburn
76. J. R. Weir, Jr.
77. G. D. Whitman
78. J. W. Woods
79. W. C. Leslie (consultant)
80. J. Moteff (consultant)
81. Hayne Palmour III (consultant)
82. J. W. Prados (consultant)
83. N. E. Promisel (consultant)
84. G. V. Smith (consultant)
85. D. F. Stein (consultant)

EXTERNAL DISTRIBUTION

86–87. ERDA DIVISION OF NUCLEAR FUEL CYCLE AND PRODUCTION, Washington, DC 20545

Director

88–89. ERDA DIVISION OF REACTOR RESEARCH AND DEVELOPMENT, Washington, DC 20545

Director

90–91. ERDA OAK RIDGE OPERATIONS OFFICE, P.O. Box E, Oak Ridge, TN 37830

Research and Technical Support Division
Director, Reactor Division

92–345. ERDA TECHNICAL INFORMATION CENTER, Office of Information Services, P.O. Box 62, Oak Ridge, TN 37830

For distribution as shown in TID-4500 Distribution Category, UC-79b (Fuels and Materials Engineering Development); UC-79h (Structural Materials Design Engineering); UC-79k (Components)